Different WASP family proteins stimulate different Arp2/3 complex-dependent actin-nucleating activities

Jonathan Zalevsky, Leah Lempert, Heather Kranitz and R. Dyche Mullins

Background: Assembly and organization of actin filaments are required for many cellular processes, including locomotion and division. In many cases, actin assembly is initiated when proteins of the WASP/Scar family respond to signals from Rho family G proteins and stimulate the actin-nucleating activity of the Arp2/3 complex. Two questions of fundamental importance raised in the study of actin dynamics concern the molecular mechanism of Arp2/3-dependent actin nucleation and how different signaling pathways that activate the same Arp2/3 complex produce actin networks with different three-dimensional architectures?

Results: We directly compared the activity of the Arp2/3 complex in the presence of saturating concentrations of the minimal Arp2/3-activating domains of WASP, N-WASP, and Scar1 and found that each induces unique kinetics of actin assembly. In cell extracts, N-WASP induces rapid actin polymerization, while Scar1 fails to induce detectable polymerization. Using purified proteins, Scar1 induces the slowest rate of nucleation. WASP activity is 16-fold higher, and N-WASP activity is 70-fold higher. The data for all activators fit a mathematical model in which one activated Arp2/3 complex, one actin monomer, and an actin filament combine into a preactivation complex which then undergoes a first-order activation step to become a nucleus. The differences between Scar and N-WASP activity are explained by differences in the rate constants for the activation step. Changing the number of actin binding sites on a WASP family protein, either by removing a WH2 domain from N-WASP or by adding WH2 domains to Scar1, has no significant effect on nucleation activity. The addition of a three amino acid insertion found in the C-terminal acidic domains of WASP and N-WASP, however, increases the activity of Scar1 by more than 20-fold. Using chemical crosslinking assays, we determined that both N-WASP and Scar1 induce a conformational change in the Arp2/3 complex but crosslink with different efficiencies to the small molecular weight subunits p18 and p14.

Conclusion: The WA domains of N-WASP, WASP, and Scar1 bind actin and Arp2/3 with nearly identical affinities but stimulate rates of actin nucleation that vary by almost 100-fold. The differences in nucleation rate are caused by differences in the number of acidic amino acids at the C terminus, so each protein is tuned to produce a different rate of actin filament formation. Arp2/3, therefore, is not regulated by a simple on-off switch. Precise tuning of the filament formation rate may help determine the architecture of actin networks produced by different nucleation-promoting factors.

Address: Department of Cellular and Molecular Pharmacology, University of California-San Francisco, San Francisco, California 94143, USA.

Correspondence: R. Dyche Mullins
E-mail: dyche@mullinslab.ucsf.edu

Received: **8 May 2001**
Revised: **16 August 2001**
Accepted: **11 October 2001**

Published: **11 December 2001**

Current Biology 2001, 11:1903–1913

0960-9822/01/$ – see front matter

Introduction

Eukaryotes use a dynamic actin cytoskeleton for many processes, including cell division, phagocytosis, intracellular trafficking, and cell locomotion [1, 2]. In response to cellular signaling events, including the activation of Rho family G proteins, cells construct specialized networks of actin filaments. The first step in de novo nucleation of actin filaments is localization and activation of the actin-nucleation machinery. The nucleation machinery consists of the Arp2/3 complex, a heteromeric complex of seven polypeptides that nucleates and crosslinks actin filaments, and a nucleation-promoting factor that binds the Arp2/3 complex and increases its nucleation activity [3]. The most well-studied nucleation-promoting factors are proteins of the WASP/Scar family [4–6]. In vertebrates, this group consists of the Wiskott-Aldrich syndrome protein

(WASP), its more widely expressed cousin, N-WASP, and at least three homologs of the *Dictyostelium* suppressor of cAMP receptor (Scar) protein, Scar1-3. The C-terminal regions of the WASP family proteins (WA regions) contain either one (WASP and Scar) or two (N-WASP) actin monomer binding domains, called WASP-homology 2 (WH2) domains [7], and a stretch of acidic residues (A) at the extreme C terminus that interacts directly with the Arp2/3 complex [8]. These WA regions are sufficient to stimulate Arp2/3-dependent actin polymerization, but the molecular details of the nucleation process remain a mystery. The WA regions are quite similar, and it has been generally assumed that their activities are equivalent.

We show here that the WASP/Scar family proteins induce conformational change(s) in Arp2/3, and in vitro WA domains from different WASP/Scar family proteins initiate dramatically different kinetics of actin polymerization. The maximal nucleation activity is determined by the acidic Arp2/3 binding region, not by the number of actin binding WH2 domains or by the affinity of the activator. We constructed a mathematical model to both describe the mechanism of Arp2/3 activation and to provide a convenient metric for Arp2/3 activity. We incorporated all of the measured rate and equilibrium constants for the interactions between actin, Arp2/3, and the WASP family proteins along with an additional activation step. The model contains only three floating parameters and more accurately describes Arp2/3-dependent polymerization than a previously proposed model based on barbed-end branching [9]. The observed differences between the activities of Scar1 WA and N-WASP WA domains can be accounted for by varying the rate constant governing the activation step.

Results

WASP and N-WASP stimulate Arp2/3-dependent actin polymerization much more rapidly than Scar1

We tested the ability of N-WASP WWA (a construct containing both WH2 domains) and Scar1 WA (a construct containing only one) to stimulate actin polymerization in *Acanthamoeba* extracts doped with pyrene actin. Previous studies have shown that the addition of GTPγS to these extracts stimulates actin polymerization [10] via the activation of Rho family GTPases. N-WASP WWA induces actin polymerization even more efficiently than GTPγS (Figure 1a). However, no amount of added Scar1 WA induces detectable polymerization.

To understand the differences between N-WASP and Scar1, we directly compared the abilities of the proteins to induce Arp2/3-dependant actin polymerization using purified proteins. At saturating concentrations, the maximal activities of N-WASP WA, WASP WA, and Scar1 WA are significantly different (Figure 1b,c). With 50 nM Arp2/3 and 2 μM actin, the time to half-maximal polymerization ($t_{1/2}$) at saturation is 42 s for WASP WA, 29 s for N-WASP WA, and 147 s for Scar1 WA (Figure 1c). The correct metric for nucleation activity is the rate at which new filaments are formed, so we determined the time course of filament generation stimulated by the three proteins (Figure 1d). We calculated the number of growing filament ends at different points in a polymerization reaction (Figure 1b) from the instantaneous slope and concentration of unpolymerized actin and then plotted barbed-end concentration versus time (Figure 1d).

WASP and N-WASP generate approximately four times as many filaments over the course of a polymerization reaction as Scar1 (Figure 1d). The initial rates of nucleation in the presence of WASP and N-WASP, however, are much more than four times the rate induced by Scar1. In the presence of WASP and N-WASP, the polymerization reaction comes to plateau within 60 s, while Scar1 does not generate a detectable number of filaments for more than 50 s.

Because Arp2/3 requires filamentous actin for maximal activity, it is formally possible that the difference in polymerization kinetics is caused by a different dependence on preformed actin filaments. To address this, we used fluorescence microscopy and measured the degree of Arp2/3-dependent filament branching in the presence of Scar1 WA and N-WASP WA. If N-WASP activity is more rapid because it can generate new filaments without a preexisting mother filament, we would expect N-WASP WA activity to produce less filament branching than Scar1 WA. In contrast, we find that N-WASP WA induces a slightly higher degree of filament branching (see Figure S1 in the Supplementary material available with this article online). In particular, N-WASP generates a significantly larger number of highly branched structures containing two or more branches each. This is consistent with N-WASP stimulating filament formation by a more rapid filament-dependent mechanism. We fluorescently labeled and imaged filaments produced by N-WASP and Scar1 WA at times when the reactions contained equal polymer mass. The reduced branching in the presence of Scar1 WA, therefore, may reflect increased debranching at the longer time required for Scar1 to generate the same polymer mass as N-WASP. Also, the slower activity of Scar1 means that spontaneous nucleation makes a larger relative contribution to filament number.

Arp2/3-dependent filament formation is not a linear function of time, so it is difficult to quantitatively compare the initial nucleation rates. To better understand the nucleation reaction and to obtain a more satisfying quantitative comparison of the activities of nucleation-promoting factors, we constructed a mathematical model of Arp2/3-dependent nucleation (Figure 2). Our model requires the assembly of one actin monomer, one nucleation-promot-

Figure 1

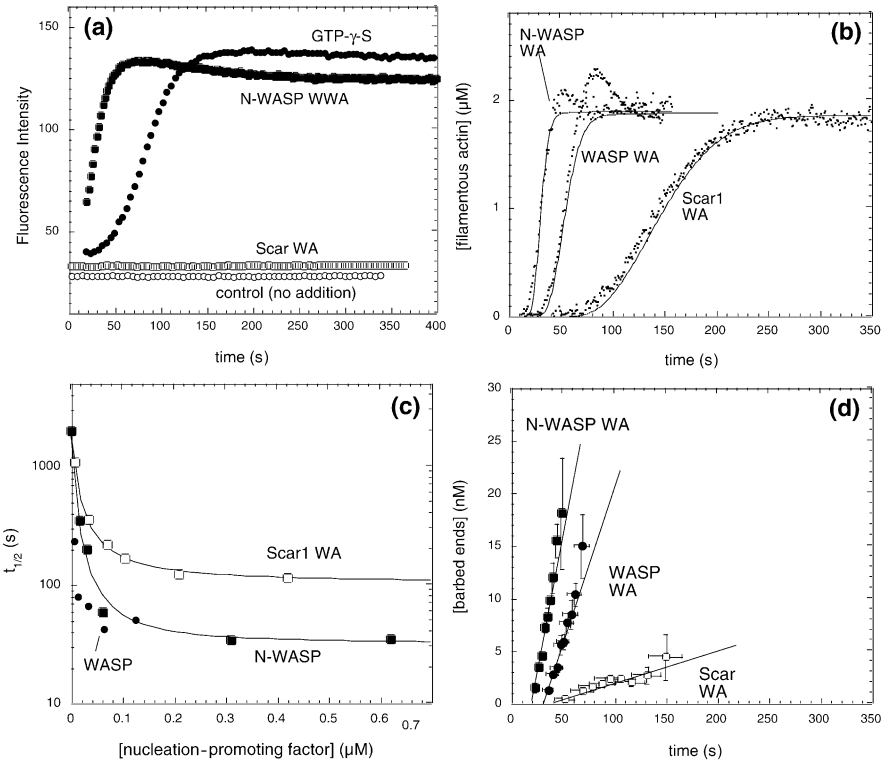

WASP family proteins induce dramatically different kinetics of actin nucleation in cell extracts and with purified components. **(a)** The addition of N-WASP WWA to *Acanthamoeba* extract induces actin polymerization similar to GTPγS, but the addition of Scar1 WA does not. Extracts were diluted 1:10 into buffer doped with 4.5 μM pyrene actin and either no activator (open circle), 200 μM GTPγS (solid circle), 115 nM Scar1 WA (aa 438–559) (open square), or 110 nM N-WASp WWA (aa 400–501) (solid square). Conditions: dilution buffer: 50 mM KCl, 1 mM $MgSO_4$, 1 mM EGTA, 1 mM DTT, 1.0 mM ATP, and 10 mM imidazole (pH 7.0); temperature: 25°C. **(b)** The maximal activity of WASP WA and N-WASP WA is faster than the maximal activity of Scar1 WA. Identical pyrene actin polymerization reactions were carried out using 2 μM actin (10% pyrene labeled) and 50 nM Arp2/3 complex with either 280 nM Scar1 WA (aa438–559) (solid square), 310 nM N-WASP WA (aa422–501), or 310 nM WASP WA (aa418–502). The points indicate polymerization data, and solid lines are fits to the kinetic model shown in Figure 2 using rate constants from Tables 1 and 2. Polymerization conditions: buffer: 50 mM KCl, 1 mM $MgCl_2$, 1 mM EGTA, 1 mM DTT, 0.2 mM ATP, and 10 mM imidazole (pH 7.0); temperature: 25°C. **(c)** Time to half-maximal polymerization of 2 μM actin with 50 nM Arp2/3 and either WASP WA (solid circle), N-WASP WA (solid square), or Scar1 WA (open square) as a function of activator concentration. At saturating concentrations, the half-times are ~5 s for N-WASP WA, ~42 s for WASP WA, and ~120 s for Scar1 WA. **(d)** The time course of Arp2/3-dependent filament formation in the presence of N-WASP WA (solid square), WASP WA (solid circle), and Scar1 WA (open square). Polymerization curves similar to those in (a) were analyzed by plotting the concentration of actin filaments versus time. Data from three separate polymerization experiments were averaged for each condition. The error bars represent the standard deviation.

ing factor, and one Arp2/3 complex on the side of an actin filament. This assumption is justified since Arp2/3 is monomeric, binds to the sides of preexisting actin filaments [11], and nucleates new daughter filaments from these mother filaments [4, 12, 13]. Also, the nucleation-promoting factors used in these studies are monomeric and contain an actin monomer binding site required for activity [7]. Our data and those of Marchand et al. [14] suggest that assembly of these components is insufficient for filament formation and that an additional activation step is required. We modeled this activation step as a first-order conversion of the assembled nucleation machinery into a stable barbed end (Figure 1e). Once formed, stable ends elongate rapidly, so we approximate that the activation step is irreversible (this is a standard assumption in modeling of both actin and microtubule nucleation [15]). To describe the entire time course of polymerization, we coupled our nucleation model to a multistep model of spontaneous polymerization described earlier [12].

We used independently determined values for all parameters in the model, except three: the rate constant describing the activation step and the forward and reverse rate constants for binding of the Arp2/3 activator-actin complex to actin filaments. Marchand et al. [14] suggested that the binding of WASP increases the affinity of Arp2/3

Figure 2

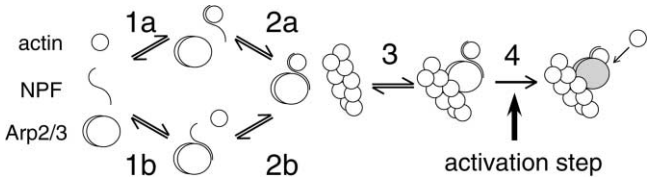

A schematic representation of the mathematical model for dendritic nucleation used in this study. First, a ternary complex is assembled between Arp2/3, actin, and a nucleation-promoting factor (NPF). This complex can assemble via one of two pathways, 1a and 2a or 1b and 2b. The ternary complex binds to the side of an actin filament (3) and undergoes a first-order activation reaction that converts it into an actin nucleus (4). This model with the parameters in Tables 1 and 2 was used to fit the polymerization data in Figure 1b and in the Supplementary material (Figure S2). The activation step is the point at which nucleation activity is regulated (see Table 2).

for actin filament, and we suspect that binding of an actin monomer increases the affinity even further. We determined values for these constants by global fitting of data sets collected with various Arp2/3 activators at different actin concentrations (Table 1; Figures 1b and S2a,c,e). The different activities of N-WASP WA, WASP WA, and Scar1 WA can be accounted for by varying a single parameter, the activation rate constant, k_{act}. We, therefore, used k_{act} as a metric to describe differences between the activities of nucleation-promoting factors. The activation rate constant for Scar1-induced nucleation is 5×10^{-4}sec^{-1}. WASP-induced nucleation is 15-fold more rapid, and N-WASP-induced nucleation is 70-fold more rapid (Figure 1b and Table 2).

The number of actin monomers bound by a nucleation-promoting factor is not a significant determinant of activity in vitro

The active domains of N-WASP WA and Scar1 WA used above (Figures 1 and 2) each contain one actin binding WH2 domain. Full-length N-WASP, however, contains two WH2 domains, so we asked whether the additional actin binding site further increases the activity of N-WASP. We directly examined the role of the additional WH2 domain in two ways; first, we fused the WA domain of Scar1 to an additional WH2 domain either from Scar1 or N-WASP (Figure 3a). Pointed-end elongation assays suggest that the chimeric proteins bind two actin monomers (Figure S3). We tested the maximal nucleating activities of saturating concentrations of the chimeric proteins and found that additional actin binding sites do not increase maximal activity (Figure 3b). Second, we compared the activities of N-WASP WWA and N-WASP WA. Using pointed-end elongation assays, we determined that N-WASP WWA appears to bind two actin monomers, while N-WASP WA and Scar1 WA bind one monomer each, with similar affinities (Figure 3c). Using pyrene actin assembly, we determined that N-WASP WWA is actually a less-efficient nucleation-promoting factor than N-WASP WA (Figure 3d).

Table 1

Rate constants for the mathematical model of dendritic nucleation, as seen in Figure 2.

Step	k_+	k_-	k_d	Source
1a/2b	5.5 $\mu M^{-1}s^{-1}$	3.0 s^{-1}	0.55 μM	[13, 15, 18]
1b/2a	1.0 $\mu M^{-1}s^{-1}$	0.4 s^{-1}	0.4 μM	[13, 18]
3	8.6 $\mu M^{-1}s^{-1}$	0.01 s^{-1}	1 nM	Least-squares fitting

Rate constant subscripts refer to reaction numbers in Figure 2.

Table 2

Activation rate constants for nucleation-promoting factors used in this study.

	k_{act} (s^{-1})	Fold/Scar1 WA
Scar1 WA	5×10^{-4}	1
WASP WA	0.008	16
N-WASP WA	0.034	68

The rate constants were determined by nonlinear least-squares fitting of the dendritic nucleation model (Figure 2) to curves of multiple concentrations of actin polymerized in the presence of 50 nM Arp2/3 and saturating concentrations of each factor. Conditions are the same as in Figure 1b.

The extreme C-terminal acidic domain of N-WASP is the primary determinant of rapid nucleation activity

To find determinants of rapid nucleation, we subdivided the WA regions of N-WASP and Scar1 into four stretches of 14–20 amino acids: the actin binding WH2 domain (W), a probable linker region (L), the cofilin homology domain (C), and the Arp2/3 binding acidic domain (A). We constructed N-WASP-Scar1 chimeras between these domains (Figure 4a) and tested their maximal activities at saturating concentrations. Replacement of the 15 amino acid acidic domain of Scar1 with the 20 amino acid acidic domain of N-WASP (Chimera A) is sufficient to increase the nucleation activity more than 20-fold (Figure 4a and data not shown). None of the chimeras were exactly as effective as N-WASP WA itself, suggesting that the proximal WH2 domain may contain an additional determinant of rapid nucleation.

The effect of swapping acidic domains is remarkable because their sequences are very similar and C-terminal domains of N-WASP and Scar1 have the same affinity for the Arp2/3 complex [16]. The most obvious difference is a three acidic amino acid insertion found in WASP and N-WASP, but absent in Scar1-3. We examined the role of this sequence on the nucleation rate by constructing Scar1(547 DED) WA, which has an insertion of these three acidic amino acids in the same register as WASP and N-WASP (Figure 4b). Scar1(547 DED) WA has an activity equal to that of Chimera A. Another mutation,

Figure 3

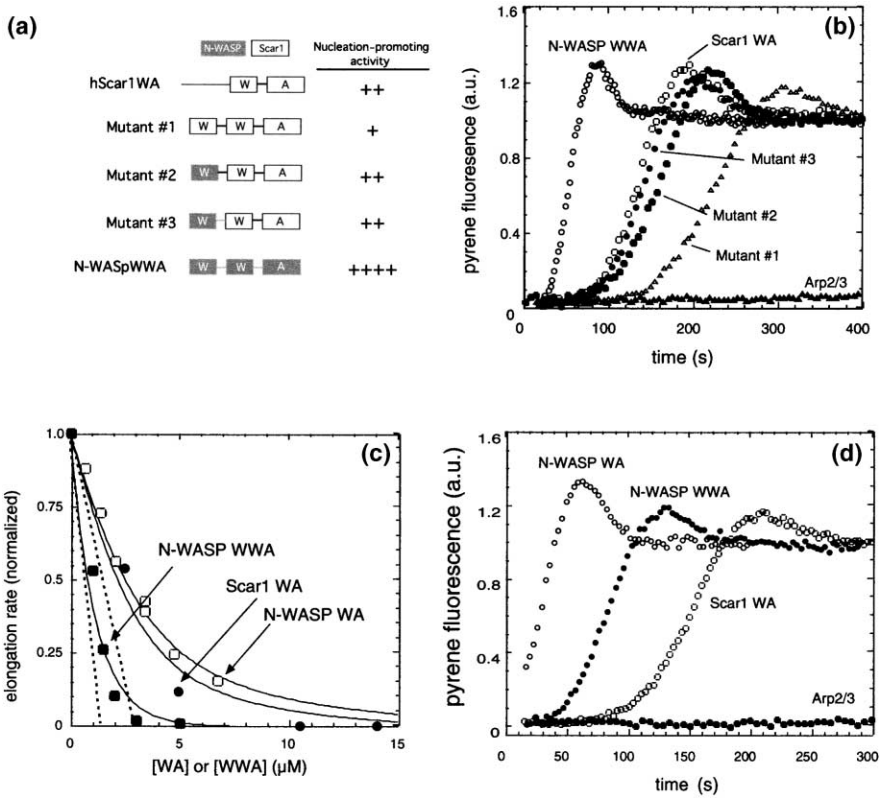

The actin monomer binding activity of N-WASP and Scar1 is not a major determinant of nucleating activity. **(a)** Chimeric Scar1 constructs with additional actin binding WH2 domains. The shaded boxes are N-WASP sequences, and dark lines and empty boxes are Scar1 sequences. Mutant #1 (Scar1 aa497–516 plus Scar1 aa487–559), Mutant #2 (N-WASP aa404–422 plus Scar1 aa497–559), Mutant #3 (N-WASP aa404–432 plus Scar1 aa487–559); (W): WH2 domain, (A): acidic domain. The symbols at the right indicate maximal activity at saturating concentrations for each protein. **(b)** Additional WH2 domains do not increase the maximal activity of Scar1 WA. Pyrene actin polymerization reactions carried out using 2 μM actin (10% pyrene) and 50 nM Arp2/3 complex alone (solid triangle), or with either 520 nM Scar1 WA (open square), 1.8 μM Mutant #1 (open triangle), 1.8 μM Mutant #2 (solid square), 1.8 μM Mutant #3 (solid circle), or 375 nM N-WASP WWA (open circle). Polymerization conditions: buffer: 50 mM KCl, 1 mM $MgSO_4$, 1 mM EGTA, 1 mM DTT, 0.2 mM ATP, and 10 mM imidazole (pH 7.0); temperature: 25°C. **(c)** Comparison of actin monomer binding by N-WASP WWA, N-WASP WA, and Scar1 WA protein constructs. Pointed-end elongation assays were carried out in the presence of varying concentrations of N-WASP WWA (solid square), N-WASP WA (open square), and Scar1 WA (solid circle). Solid lines are curves fit to the data. Dashed lines are theoretical curves representing infinitely tight binding to either one (right line) or two (left line) actin monomers. Polymerization reactions and data analysis were carried out as described previously [16]. **(d)** Removal of the N-terminal WH2 domain increases the maximal activity of N-WASP in vitro. Pyrene actin polymerization reactions contained 2 μM actin (10% pyrene), 50 nM Arp2/3 complex, and either 520 nM Scar1 WA (aa438–559) (open square), 375 nM N-WASP WWA (aa400–501) (solid circle), or 310 nM N-WASP WA (aa422–501) (open circle). Conditions are the same as in (b).

conversion of leucine 558 to glutamic acid produces a smaller but reproducible increase in activity. We conclude that the three acidic amino acid insertion at position 547 accounts for most of the effects of swapping acidic domains (Figure 4c).

Both N-WASP and Scar1 induce a conformational change in the Arp2/3 complex

The results above are consistent with a model in which the nucleation-promoting factors stimulate Arp2/3 activity by an allosteric mechanism. We looked for conformational changes within the Arp2/3 complex by chemical crosslinking with EDC/NHS. To better characterize intramolecular crosslinks, we raised polyclonal antibodies against the p14 and p18 subunits of the *Acanthamoeba* Arp2/3 complex. Together with our previously described antibodies against Arp2, Arp3, p40, and p35 [11, 17], the new reagents allow for more accurate identification of crosslinked Arp2/3 subunits.

Upon binding, N-WASP WWA and Scar1 WA induce formation of a new intramolecular crosslink in the Arp2/3 complex. We first detected the crosslinked species as a new band recognized by monospecific antibodies against the p18 subunit (Figure 5a, band 1) that does not bind

Figure 4

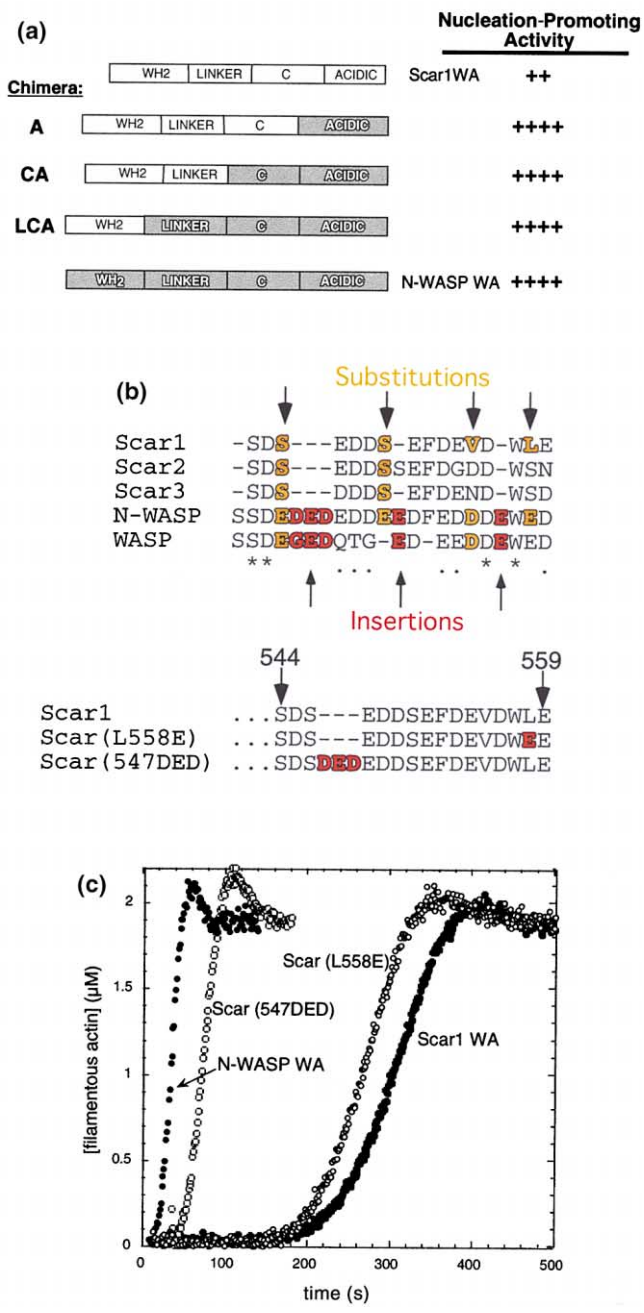

The acidic domain of N-WASP is the major determinant of maximal nucleation activity. **(a)** N-WASP/Scar1 chimeras used in this study. Scar1 WA and N-WASP WA were subdivided into four segments: WH2, a LINKER region, a C segment that includes the cofilin homology domain, and the extreme C-terminal ACIDIC domain. Three chimeras were constructed between the N-WASP and Scar1 versions of these segments: Chimera A (Scar1 aa497–544 plus N-WASP aa484–501), Chimera CA (Scar1 aa497–528 plus N-WASP aa468–501), and Chimera LCA (Scar1 aa497–514 plus N-WASP aa450–501). The shaded boxes represent N-WASP sequences, and the clear boxes represent Scar1 amino acids. The table on the right shows the maximal activity at saturating concentrations for each protein. **(b)** Alignment of the acidic domains of several WASP family proteins. WASP and N-WASP contain a conserved insertion of three amino acids (shaded amino acids) not found in the Scar proteins. The acidic domain of Scar1(547 DED) WA is also shown. **(c)** Insertion of the three acidic amino acids (DED) at Scar1 position 547 increases the nucleation rate of Scar1 WA. Pyrene actin assembly assays contained 2 μM actin (10% pyrene labeled), 50 nM Arp2/3 complex with either 520 nM Scar1 WA (solid square), 520 nM Scar1(L558E) WA (open circle), 430 nM Scar1(547 DED) WA (open square), or 310 nM N-WASP WA (solid circle). Polymerization conditions are the same as in Figure 1b.

monoclonal anti-his$_6$ antibodies that recognize the affinity tag on Scar1 WA and N-WASP WWA. Therefore, this band appears to be a specific intramolecular crosslink within the Arp2/3 complex that occurs only upon binding of N-WASP or Scar1. The crosslinked band is also not recognized by antibodies against Arp3, Arp2, p40, p35, or p14. Therefore, it represents either an intrasubunit crosslink that dramatically alters the electrophoretic mobility of p18 or an intersubunit crosslink between p18 and p19 (for which we do not have a monospecific antibody). A p18/p19 crosslink is consistent with previous two-hybrid results [8], so we propose that, upon binding, N-WASP WWA and Scar1 WA induce a conformational change in the Arp2/3 complex that brings crosslinkable residues of p18 and p19 into contact.

N-WASP and Scar1 crosslink to different small molecular weight subunits of the Arp2/3 complex

As reported previously, the binding site for N-WASP WWA and Scar1 WA involves contacts with the Arp2, Arp3, and p40 subunits of the Arp2/3 complex [16]. N-WASP WWA and Chimera A, both of which initiate rapid filament formation, crosslink to p14 (Figure 5a, band 4, and Figure 5b) and p18 (Figure 5a, band 3, and Figure 5b). The relative intensity of band 3 is different when probed with the anti-his$_6$ or the anti-p18 antibodies. This difference probably reflects a change in the accessibility of the epitopes for the p18 antibody in the p18/N-WASP WWA crosslink.

Scar1 crosslinks to the p18 subunit but does not detectably crosslink to p14. In a previous study, we did not detect a connection between Scar1 and p18 [16]. Reliable detection of this interaction was made possible by our new antibodies and supports a previous study that found an association between Scar1 WA and the p21ARC subunit (the mammalian homolog of amoeba p18) of the mammalian Arp2/3 complex in a yeast two-hybrid screen [8].

Discussion

One of the major conclusions of this study is that the nucleation activity of the Arp2/3 complex can be tuned to different values by different WASP family proteins. N-WASP WA stimulates actin polymerization in *Acanthamoeba* extracts and, in assays with components purified from *Acanthamoeba*, promotes rapid actin nucleation fol-

Figure 5

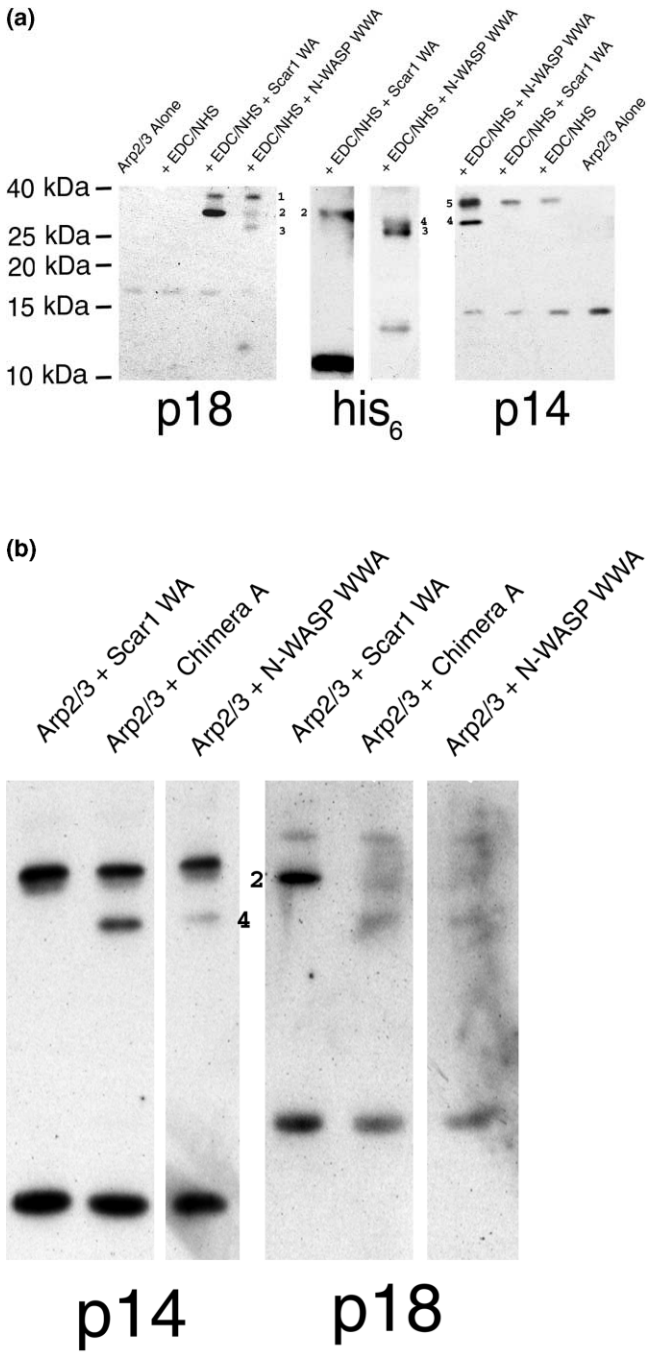

N-WASP WWA and Scar1 WA induce a conformational change in the Arp2/3 complex. **(a)** Band 1 is a new intramolecular crosslink between the p18 and p19 subunits that does not contain N-WASP or Scar1 but only appears when these proteins interact with the Arp2/3 complex. N-WASP WWA and Scar1 WA have different associations with the p14 and p18 subunits. Scar1 WA associates strongly with the p18 subunit of the Arp2/3 complex (band 2), whereas N-WASP WWA makes a weak contact (band 3). N-WASP WWA interacts with the p14 subunit of the Arp2/3 complex (band 4), while Scar1 WA fails to associate with this subunit. Band 5 is a previously described intramolecular crosslink between the p14 and p19 subunits of the Arp2/3 complex [11]. Crosslinking reaction conditions: 2 mM EDC/NHS (50 mM KCl, 1 mM $MgSO_4$, 1 mM EGTA, 1 mM DTT, 0.2 mM ATP, and 10 mM imidazole [pH 7.0]) was added to 1 μM Arp2/3 complex alone or with either 12 μM Scar1 WA or 5 μM N-WASP WWA for 45 min at room temperature. **(b)** Replacing the acidic domain of hScar1 with that of N-WASP produces the same pattern of chemical crosslinks as N-WASP WWA. A total of 345 nM Arp2/3 complex was mixed with either 4 μM Scar1 WA, 4.4 μM Chimera A, or 2 μM N-WASP WWA under the same conditions as in (a). Chimera A and N-WASP both crosslink to the p14 subunit of the Arp2/3 complex and fail to make a strong contact with the p18 subunit.

lowing a short lag time. Scar1 WA stimulates a 70-fold slower rate of nucleation in vitro and is unable to stimulate actin polymerization in extracts. This difference is not due to a different dependence on preformed actin filaments, but it appears to be a difference in the kinetics of the nucleation reaction. Previously [10], we showed that, because of filament capping, the number of free barbed ends in amoeba extracts is directly proportional to the rate of nucleation, so we conclude that the maximal nucleation rate initiated by Scar1 WA cannot overcome filament capping and disassembly activities in amoeba extracts.

Yamaguchi et al. [18] noted a similar difference in the activities of N-WASP WWA and Scar1 WA but attributed it to the difference in the number of actin binding sites. That study, however, did not compare the activity of an N-WASP WWA construct, containing two actin binding sites, to an N-WASP WA construct, which contains only one. In the present study, this control experiment (Figure 3d) rules out the number of actin binding sites as a determinant of rapid nucleation by N-WASP WA. Yamaguchi et al. [18] report that the addition of WH2 domains to Scar1 WA enhances nucleation activity, a result that disagrees with our findings. Several technical differences could account for this. First, the proteins used in our study are untagged or tagged with six histidines, while the proteins used in the Yamaguchi study were fused to glutathione-S-transferase (GST). Higgs et al. [19] showed that WASP family protein constructs fused to GST have significantly different activities compared to untagged proteins. Also, GST fusion proteins are generally dimers, so a GST-WWA construct could potentially bind four actin monomers and two molecules of Arp2/3, further confusing the relationship between nucleation and actin binding. Second, the two studies use different linker sequences between WH2 domains (see the legend to Figure 3a,b). To make a Scar1 WWA construct, Yamaguchi et al. fused amino acids 466–519 to amino acids 494–559. In the present study, we built an analogous construct by fusing amino acids 497–516 to amino acids 487–559. We chose these boundaries to maintain the spacing between WH2 domains found in N-WASP. We also tested the C-terminal WH2 domain and linker sequence from N-WASP and used a quantitative assay (pointed-end elongation) to verify that our WWA constructs bind two actin monomers (see the Supplementary material, Figure S3). Third, in the present study, we used saturating concentrations of Scar1 (W)WA proteins, so that our comparison of nucleation activities was insensitive to the affinity of the constructs for Arp2/3. Yamaguchi et al. used 100 nM N-WASP/Scar1 (W)WA and 60 nM Arp2/3 complex. In our experiments, 100 nM N-WASP or Scar (W)WA is not sufficient to saturate the activity of 60 nM Arp2/3 complex. So, one possibility is that the apparent difference in activities between the Scar1 WA and WWA constructs used by Yamaguchi et al. is actually due to a difference in their affinities for Arp2/3.

Several metrics have been used to describe the nucleation activity of the Arp2/3 complex, including the time to half-maximal polymerization [16], the total number of actin filaments generated during an assay [14], and the maximal rate of polymerization [20]. Each suffers from drawbacks that limit its use for quantitative comparisons. The time to half-maximal polymerization is a model-independent metric useful for plotting dose curves and determining relative nucleation activities but cannot be used for absolute quantitative comparisons. The total number of filaments generated in a polymerization assay is limited by the depletion of actin monomers and is not linear with time. Consequently, the total number of filaments generated in a polymerization assay is not proportional to the nucleation rate. This is most clearly seen in Figure 1d, in which the total number of filaments generated by N-WASP is only four times greater than that generated by Scar1. At early time points, however, say 0–50 s, the difference in filament numbers is clearly much greater. The appropriate model-independent metric of nucleation activity is, therefore, not total filament number but the rate of filament formation (Figure 1d). Comparisons based on the maximal polymerization rate suffer from a similar problem.

A previous study [13] reported no significant difference in the activities of WASP WA and Scar1 WA. The authors compared the activity of bovine Arp2/3 stimulated with WASP WA to that of *Acanthamoeba* Arp2/3 stimulated with Scar1, so comparison was not direct. Also, the authors used total filament number as a metric of activity and found that, depending on Arp2/3 concentration, Scar1 WA stimulation produced 50%–80% as many filaments as WASP WA. According to our analysis, a 2-fold difference in filament number can correspond to a much higher difference in the rate of filament formation. So, while our observations are not inconsistent with those of Blanchoin et al., our analysis indicates a larger difference in the activities of Scar1 and WASP than these authors appreciated.

To better quantitate Arp2/3 activity, we constructed a complete kinetic model of Arp2/3-dependent filament formation. Nucleation by activated Arp2/3 requires one molecule each of Arp2/3 and nucleation-promoting factor, an Arp2/3 binding site on the side of a filament, and an actin monomer. The model fits the data well at multiple Arp2/3 and actin concentrations and provides a metric, the activation rate constant, for quantitatively comparing the activities of different nucleation-promoting factors. Unlike other metrics discussed, our model-based metric is largely independent of assay conditions (e.g., the concentrations of actin and Arp2/3) and can be used to com-

pare results from different laboratories and different nucleation-promoting factors.

A model proposed by Pantaloni et al. [9] suggests that three actin monomers are required for Arp2/3-dependent nucleation. We tested this branched polymerization model against our mathematical model of dendritic nucleation (see the Supplementary material). The branched polymerization model can accurately fit data collected at varying Arp2/3 concentrations [9] but cannot fit either spontaneous or Arp2/3-mediated actin polymerization at varying actin concentrations (see the Supplementary material, Figure S2b,d,f). Three factors contribute to this failure; first, spontaneous nucleation is modeled as actin dimerization, and all filaments are treated as actin dimers in equilibrium with monomers. This disagrees with previous work indicating that the critical nucleus for actin polymerization is a trimer [21, 22] and means that the dimerization rate constants in the model have no clear physical meaning. Second, the branched polymerization model proposes that three actin monomers combine with Arp2/3 to make a new daughter filament. This gives the Arp2/3-dependent nucleation reaction a third-order dependence on the actin monomer concentration, which appears to be much too high. And, third, the branched polymerization model does not contain a separate activation step. A first-order activation step following the assembly of Arp2/3, activator, and actin decreases the dependence of the nucleation rate on actin and Arp2/3 at high concentrations. Pantaloni et al. [9] also noted that the specific activity of Arp2/3 decreased at high concentrations but proposed that a complex of Arp2/3, N-WASP WA, and an actin monomer self-associates to form a nonproductive dimer. There is no experimental evidence for this, while inclusion of a first-order activation step is supported by available data [14].

Nucleation requires an activation step that can be separated from actin and Arp2/3 binding (Figure 2). Three lines of evidence suggest that this step represents a conformational change on the Arp2/3 complex. First, by chemical crosslinking, we detect a shift in Arp2/3 subunit interactions upon binding of Scar1 and N-WASP. Second, differences in nucleation activity are not correlated with differences in affinity for Arp2/3 or actin. And, third, sequence differences that alter the kinetics of nucleation lie within the Arp2/3 binding site and affect crosslinking to Arp2/3 subunits. If tethering an actin monomer to Arp2/3 was sufficient for nucleation, we would expect mutations affecting activity to either alter the affinity for actin or Arp2/3 or to affect the geometry and flexibility of the tether. Based on our data, we suggest that the activation step is a conformational change on Arp2/3 and that the number of acidic residues at the C terminus of WASP family proteins determines the stability of the active conformation.

Intracellular pathogens that spread from cell to cell by recruiting components of the host cell cytoskeleton may have already discovered the difference between N-WASP and Scar1. Vaccinia virus and *Shigella* recruit N-WASP [23, 24], and *Listeria monocytogenes* uses ActA [25, 26], which has a nucleation activity indistinguishable from that of N-WASP [16]. To date, no intracellular pathogen has been found to recruit Scar1 or express a factor with Scar1-like activity. The rate of filament formation stimulated by a nucleation-promoting factor may be a significant determinant of its use in actin-based pathogen motility.

Why have cells evolved multiple nucleation-promoting factors that stimulate different rates of Arp2/3-dependent actin filament formation? We propose that the rate of actin filament formation initiated by the Arp2/3 complex plays a role in determining the three-dimensional architecture of an actin-based structure. Several studies have shown that the expression of different nucleation-promoting factors produces different effects on cell morphology and the organization of the actin cytoskeleton [27, 28]. It is unclear how many of these differences are due to activation of collateral signaling pathways or recruitment of nonidentical sets of actin binding proteins and how many are due to intrinsic differences in the activity of the nucleation machinery. The relationship between actin network architecture and the dissociation rates of actin crosslinking proteins has been well studied [29, 30], but the connection between filament nucleation rate (especially in the presence of crosslinking proteins) and network architecture is still mysterious. Evidence for a connection between nucleation rate and cellular architecture has come from the study of mutations associated with human disease. Derry et al. [31] found that mutation of arginine 477 of WASP to lysine is associated with thrombocytopenia. Marchand et al. [14] report that this mutation does not alter the affinity for Arp2/3, but decreases nucleation-promoting activity. In that study, WASP WA (R477K) generated half as many filaments as wild-type WASP WA. According to our kinetic model, this decrease in filament number probably corresponds to a 10-fold decrease in the nucleation rate. WASP (R477K), therefore, should still nucleate filaments as rapidly as Scar1. The effect of the WASP (R477K) mutation in vivo suggests that a higher nucleation rate is essential for proper function of WASP. The specific determinants of actin network architecture in vivo obviously require further study.

Materials and methods

Protein purification

All Scar1, WASP, N-WASP, and chimeric proteins were constructed by PCR with a proofreading polymerase using human Scar1, human WASP, and rat N-WASP as templates. All clones were verified by sequencing. Scar1 WA (aa438–559) was expressed with a C-terminal his_6 tag that was left intact in the purified protein. Scar1 WA (aa443–559) was expressed as a GST fusion protein and was purified by standard methods. The GST tag was removed by protease digestion, and the cleaved product was further purified by either gel filtration on Superdex-

S200 or by chromatography on MonoQ resin (Pharmacia). For MonoQ purification, we loaded protein onto the resin in 10 mM Tris (pH 8.0), 1 mM DTT and eluted with a gradient of 0–0.5 M KCl. Cleaved Scar WA eluted as a single symmetrical peak between 390–430 mM KCl. Using mass spectrometry, we determined that the protein was 13,077 Da, close to the predicted molecular mass of 13,061 Da. We saw no difference in activity between Scar WA purified by glutatione affinity alone or in combination with the additional chromatographic steps (unpublished data). N-WASP WWA (aa400–501) was expressed with an N-terminal his_6 tag that was removed by protease digestion following protein purification. The WH2-addition protein constructs were expressed with C-terminal his_6 tags and were purified by standard methods. WASP WA (aa418–502), N-WASP WA (aa422–501), and N-WASP WA/Scar1WA protein chimeras were expressed as GST fusions and were purified by standard methods. The GST tag was removed by protease digestion.

Arp2/3 from *Acanthamoeba castellani* was purified either by conventional chromatography, as described previously [9, 16, 32], or by a combination of conventional and affinity chromatography. In the second purification scheme, *Acanthamoeba* were lysed by N_2 cavitation in sucrose lysis buffer (5 mM dithiothreitol [DTT], 1 mM ATP, 2 mM EGTA, 0.5 mM benzamidine, 1 mM phenyl-methyl-sulfonyl fluoride [PMSF], 0.2 M sucrose, 20 mM Tris [pH 8.0]), centrifuged at low (10,000×g for 15 min) and high (140,000×g for 1 hr), and chromatorgaphed sequentially on DEAE cellulose (Whatman) and C-200(m) (Millipore) preequilibrated with 10 mM Tris (pH 8.0), 0.5 mM DTT, 1 mM ATP, 0.1 mM $CaCl_2$. Arp2/3 binds to neither resin at pH 8.0, so we loaded the flowthrough onto an N-WASP-affinity matrix made by coupling his_6-tagged N-WASP WA to CH-Sepharose by standard methods. The column was washed with 20–50 column volumes and then eluted with 0.5 M KCl. Eluate was then passed over phenyl-sepharose resin to remove remaining contaminants. Arp2/3 purified by the second protocol was measurably more active than Arp2/3 purified solely by conventional chromatography. For this reason, we used Arp2/3 purified by this protocol for almost all experiments in the paper. The exception is experiments shown in Figure 3 for which we used Arp2/3 purified by conventional chromatography.

Actin was purified according to [33] and [12] and was pyrene labeled as described in [34]. *Acanthamoeba* extract used in polymerization experiments was prepared as in [10].

Actin polymerization

Actin polymerization assays were preformed according to [16] using the protein concentrations and conditions specified in the figure legends. Raw fluorescence data were converted to concentrations of polymeric actin, and data sets were corrected for instrumental and assay dead time. Pointed-end elongation assays were carried out using gelsolin-actin dimers as seeds [12]. The concentration of filament barbed ends was calculated as described previously [35]. Data were obtained using a K2 multifrequency fluorometer (ISS) and were analyzed using KaleidaGraph (Synergy Software).

Fluorescence microscopy

We polymerized 2 μM actin along with 50 nM Arp2/3 and 750 nM Scar1 WA or N-WASP WA. When reactions were 40% complete (50 s for N-WASP and 140 s for Scar1), we diluted them 1:5 into 10 μM alexa488-labeled phalloidin (Molecular Probes) and then 1:100 into microscopy buffer (10 mM imidazole [pH 7.0], 50 mM KCl, 1 mM $MgCl_2$, 0.5 mM DTT, 0.01 vol/vol Oxyrase [Oxyrase], 20 mM lactate). We loaded 5-μl aliquots onto coverslips precoated for 10 min with 5 mg/ml DEAE-dextran. We imaged labeled filaments using a Nikon TE300 quantum inverted microscope with a 100× Nikon DIC objective. We captured images with a Hammamatsu Orca II CCD camera cooled to −50°C.

Kinetic simulations

Modeling and curve fitting were performed using Berkeley Madonna v8.0 (Robert Macey and George Oster, University of California, Berkeley CA). The model for spontaneous polymerization was identical to that described in [12] and was optimized by fitting to polymerization curves. All rate constants are identical to those in [12], with the following exceptions: $k_{-1} = 2.49 \times 10^6$, and $k_{-2} = 2.32 \times 10^5$. To fit data in the presence of activated Arp2/3, we coupled the spontaneous polymerization model to the Arp2/3-mediated polymerization model in Figure 2 and varied k_{+3}, k_{-3}, and k_{act}, as described in the Results.

Arp2/3-mediated polymerization model (Figure 2): 1a, $A + N \leftrightarrow AN$; 1b, $R + N \leftrightarrow NR$; 2a, $AN + R \leftrightarrow ANR$; 2b, $A + NR \leftrightarrow ANR$; 3, $ANR + P \leftrightarrow ANRP$; 4, $ANRP \leftrightarrow F$; 5, $AN + F \rightarrow N + F$.

Symbols represent: A: actin monomer, N: nucleation-promoting factor, R: Arp2/3 complex, P: polymeric actin, F: actin filament barbed end. Reaction 5 describes the addition of WH2-bound actin monomers to free barbed ends. We chose $k_{+5} = 10\ \mu M^{-1}s^{-1}$. Together with our model of spontaneous polymerization, this reaction accounts for the experimental observation that binding of an actin monomer to a WH2 domain inhibits spontaneous nucleation but has little effect on barbed-end elongation [16, 19, 23]. Data sets and Berkeley Madonna model files described in this paper are available on request.

Antibody preparation

Acanthamoeba Arp2/3 complex was prepared as described above. The p14 and p18 subunits were resolved by SDS-PAGE, excised from the gel, and injected into chickens using the specified protocol (Covance). IgY antibodies were isolated from chicken eggs using the EggStract IgY purification kit (Promega). These IgY were further purified by gel filtration using S-300.

Chemical crosslinking

Proteins were dialyzed into 50 mM KCl, 1 mM $MgSO_4$, 1 mM EGTA, and 10 mM imidazole (pH 7.0) at 25°C to facilitate crosslinking. The indicated protein concentrations were mixed with freshly prepared 1-ethyl-3-(3-dimethylaminopropyl)-carbodiimide hydrochloride (EDC) and N-hydroxysuccinimide (NHS) for 30 min at room temperature. Samples were methanol/chloroform precipitated and analyzed by Western blotting with monospecific antibodies against the Arp2/3 complex subunits or anti-his_6 antibody to recognize the affinity tag on N-WASP WWA and Scar1 WA.

Supplementary material

Supplementary material including a comparison of mathematical models for dendritic nucleation, as described in this study, and branched polymerization as proposed by Pantaloni et al. [9] is available at http://images.cellpress.com/supmat/supmatin.http. In addition, there is a comparison of the actin binding activities of Scar1 WA and WWA constructs.

Acknowledgements

This work was supported by grants from the National Institutes of Health (GM61010-01), the Pew Charitable Trust (P0325SC), and the Human Frontiers in Science Program (RG0111/2000-M) to R.D.M. The work was also supported by a Research Resources Program grant (53000284) from the Howard Hughes Medical Institute to the UCSF School of Medicine. We are grateful to Beth Holleran, Mark Dayel, and other members of the Mullins lab for helpful discussions and to Ron Vale and Jonathan Weissman for critical reading of the manuscript. R.D.M. remembers Lloyd Mullins (1931–2001), and J.Z. expresses gratitude to Olivia Zalevsky for highly entertaining conversations.

References

1. Machesky LM: **Cell motility: complex dynamics at the leading edge.** *Curr Biol* 1997, **7:**R164-R167.
2. Taunton J: **Actin filament nucleation by endosomes, lysosomes and secretory vesicles.** *Curr Opin Cell Biol* 2001, **13:**85-91.
3. Pollard T, Blanchoin L, Mullins R: **Molecular mechanisms controlling actin filament dynamics in nonmuscle cells.** *Ann Rev BiophysBiomol Struct* 2000, **29:**545-576.
4. Machesky LM, Mullins RD, Higgs HN, Kaiser DA, Blanchoin L, May RC, *et al.*: **Scar, a WASp-related protein, activates nucleation of actin filaments by the Arp2/3 complex.** *Proc Natl Acad Sci USA* 1999, **96:**3739-3744.

5. Rohatgi R, Ma L, Miki H, Lopez M, Kirchhausen T, Takenawa T, *et al.*: **The interaction between N-WASP and the Arp2/3 complex links Cdc42-dependent signals to actin assembly.** *Cell* 1999, **97:**221-231.
6. Yarar D, To W, Abo A, Welch MD: **The Wiskott-Aldrich syndrome protein directs actin-based motility by stimulating actin nucleation with the Arp2/3 complex.** *Curr Biol* 1999, **9:**555-558.
7. Mullins R: **How WASP-family proteins and the Arp2/3 complex convert intracellular signals into cytoskeletal structures.** *Curr Opin Cell Biol* 2000, **12:**91-96.
8. Machesky LM, Insall RH: **Scar1 and the related Wiskott-Aldrich syndrome protein, WASP, regulate the actin cytoskeleton through Arp2/3 complex.** *Curr Biol* 1998, **8:**1347-1356.
9. Pantaloni D, Boujemaa R, Didry D, Gounon P, Carlier M: **The Arp2/3 complex branches filament barbed ends: functional antagonism with capping proteins.** *Nat Cell Biol* 2000, **2:**385-391.
10. Mullins RD, Pollard TD: **Rho-family GTPases require the Arp2/3 complex to stimulate actin polymerization in *Acanthamoeba* extracts.** *Curr Biol* 1999, **9:**405-415.
11. Mullins RD, Stafford WF, Pollard TD: **Structure, subunit topology, and actin-binding activity of the Arp2/3 complex from *Acanthamoeba.*** *J Cell Biol* 1997, **136:**331-343.
12. Mullins RD, Heuser JA, Pollard TD: **The interaction of Arp2/3 complex with actin: nucleation, high-affinity pointed end capping, and formation of branching networks of filaments.** *Proc Natl Acad Sci USA* 1998, **95:**6181-6186.
13. Blanchoin L, Amann KJ, Higgs HN, Marchand JB, Kaiser DA, Pollard, TD: **Direct observation of dendritic actin filament networks nucleated by Arp2/3 complex and WASP/Scar proteins.** *Nature* 2000, **404:**1007-1011.
14. Marchand JB, Kaiser DA, Pollard TD, Higgs HN: **Interaction of WASP/Scar proteins with actin and vertebrate Arp2/3 complex.** *Nat Cell Biol* 2001, **3:**76-82.
15. Flyvbjerg H, Jobs E, Leibler S: **Kinetics of self-assembling microtubules: an "inverse problem" in biochemistry.** *Proc Natl Acad Sci USA.* 1996, **93:**5975-5979.
16. Zalevsky J, Grigorova I, Mullins R: **Activation of the Arp2/3 complex by the Listeria ActA protein: ActA binds two actin monomers and three subunits of the Arp2/3 complex.** *J Biol Chem* 2001, **276:**3468-3475.
17. Kelleher JF, Atkinson SJ, Pollard TD: **Sequences, structural models, and cellular localization of the actin-related proteins Arp2 and Arp3 from *Acanthamoeba.*** *J Cell Biol* 1995, **131:**385-397.
18. Yamaguchi H, Miki H, Suetsugu S, Ma L, Kirschner M, Takenawa T: **Two tandem verprolin homology domains are necessary for a strong activation of Arp2/3 complex-induced actin polymerization and induction of microspike formation by N-WASP.** *Proc Nat Acad Sci USA* 2000, **97:**12631-12636.
19. Higgs HN, Blanchoin L, Pollard TD: **Influence of the C terminus of Wiskott-Aldrich syndrome protein (WASp) and the Arp2/3 complex on actin polymerization.** *Biochemistry* 1999, **38:**15212-15222.
20. Prehoda KE, Scott JA, Mullins RD, Lim WA: **Integration of multiple signals through cooperative regulation of the N-WASP-Arp2/3 complex.** *Science* 2000, **290:**801-806.
21. Oosawa F, Kasai M: **A theory of linear and helical aggregations of macromolecules.** *J Mol Biol* 1962, **4:**10-21.
22. Frieden C: **Polymerization of actin: mechanism of the Mg^{2+}-induced process at pH8 and 20C.** *Proc Natl Acad Sci USA* 1983, **80:**6513-6517.
23. Egile C, Loisel TP, Laurent V, Li R, Pantaloni D, Sansonetti PJ, *et al.*: **Activation of the CDC42 effector N-WASP by the shigella flexneri IcsA protein promotes actin nucleation by Arp2/3 complex and bacterial actin-based motility.** *J Cell Biol* 1999, **146:**1319-1332.
24. Moreau V, Frischknecht F, Reckmann I, Vincentelli R, Rabut G, Stewart D, *et al.*: **A complex of N-WASP and WIP integrates signalling cascades that lead to actin polymerization.** *Nat Cell Biol* 2000, **2:**441-448.
25. Smith G, Portnoy D: **How the Listeria monocytogenes ActA protein converts actin polymerization into a motile force.** *Trends Microbiol* 1997, **5:**272-276.
26. Skoble J, Portnoy D, Welch M: **Three regions within ActA promote Arp2/3 complex-mediated actin nucleation and Listeria monocytogenes motility.** *J Cell Biol* 2000, **150:**527-538.
27. Miki H, Sasaki T, Takai, Y, Takenawa T: **Induction of filopodium formation by a WASP-related actin-depolymerizing protein N-WASP.** *Nature* 1998, **391:**93-96.
28. Miki H, Suetsugu S, Takenawa T: **WAVE, a novel WASP-family protein involved in actin reorganization induced by Rac.** *EMBO J* 1998, **17:**6932-6941.
29. Wachsstock DH, Schwarz WH, Pollard TD: **Crosslinker dynamics determine the mechanical properties of actin gels.** *Biophys J* 1994, **66:**801-809.
30. Xu J, Wirtz D, Pollard TD: **Dynamic cross-linking by alpha-actinin determines the mechanical properties of actin filament networks.** *J Biol Chem* 1998, **273:**9570-9576.
31. Derry JM, Kerns JA, Weinberg KI, Ochs HD, Volpini V, Estivill X, *et al.*: **WASP gene mutations in Wiskott-Aldrich syndrome and X-linked thrombocytopenia.** *Hum Mol Genet* 1995, **4:**1127-1135.
32. Kelleher JF, Mullins RD, Pollard TD: **Purification and assay of the Arp2/3 complex from *Acanthamoeba castellanii.*** *Methods Enzymol* 1998, **298:**42-51.
33. MacLean-Fletcher S, Pollard TD: **Mechanism of action of cytochalasin B on actin.** *Cell* 1980, **20:**329-341.
34. Cooper JA, Walker SB, Pollard TD: **Pyrene actin: documentation of the validity of a sensitive assay for actin polymerization.** *J Muscle Res Cell Motil* 1983, **4:**253-262.
35. Mullins R, Machesky L: **Actin assembly mediated by Arp2/3 complex and WASP family proteins.** *Methods Enzymol* 2000, **325:**214-237.